

RESEARCH ARTICLE

Scaling and development of elastic mechanisms: the tiny strikes of larval mantis shrimp

Jacob S. Harrison^{1,*}, Megan L. Porter², Matthew J. McHenry³, H. Eve Robinson⁴ and S. N. Patek¹

ABSTRACT

Latch-mediated spring actuation (LaMSA) is used by small organisms to produce high acceleration movements. Mathematical models predict that acceleration increases as LaMSA systems decrease in size. Adult mantis shrimp use a LaMSA mechanism in their raptorial appendages to produce extremely fast strikes. Until now, however, it was unclear whether mantis shrimp at earlier life-history stages also strike using elastic recoil and latch mediation. We tested whether larval mantis shrimp (*Gonodactylaceus falcatus*) use LaMSA and, because of their smaller size, achieve higher strike accelerations than adults of other mantis shrimp species. Based on microscopy and kinematic analyses, we discovered that larval *G. falcatus* possess the components of, and actively use, LaMSA during their fourth larval stage, which is the stage of development when larvae begin feeding. Larvae performed strikes at high acceleration and speed (mean: $4.133 \times 10^5 \text{ rad s}^{-2}$, 292.7 rad s^{-1} ; 12 individuals, 25 strikes), which are of the same order of magnitude as for adults – even though adult appendages are up to two orders of magnitude longer. Larval strike speed (mean: 0.385 m s^{-1}) exceeded the maximum swimming speed of similarly sized organisms from other species by several orders of magnitude. These findings establish the developmental timing and scaling of the mantis shrimp LaMSA mechanism and provide insights into the kinematic consequences of scaling limits in tiny elastic mechanisms.

KEY WORDS: Latch-mediated spring actuation, Mantis shrimp, Larvae, Elastic mechanisms, Power amplification, Stomatopoda

INTRODUCTION

Latch-mediated spring actuation (LaMSA) mechanisms generate extremely high accelerations in jellyfish nematocysts, trap-jaw ant mandibles and the raptorial appendages of mantis shrimp (Longo et al., 2019; Nüchter et al., 2006; Gronenberg, 1996; Larabee et al., 2017; Patek et al., 2004; McHenry et al., 2016). LaMSA mechanisms achieve their impressive kinematics using motors, springs and latches that mediate the storage and release of elastic energy (Longo et al., 2019). Biological LaMSA mechanisms outperform engineered systems and their study has advanced understanding of the physics underlying elastic energy storage and release (Ilton et al., 2018; Olberding et al., 2019; Liang and Crosby, 2020). LaMSA has evolved independently across numerous clades

and is used primarily by small organisms, when the accelerated mass is less than a kilogram (Ilton et al., 2018; Sakes et al., 2016; Sutton et al., 2019).


Mathematical models of LaMSA scaling predict that structures of smaller size can achieve greater acceleration (Ilton et al., 2018). Comparisons of LaMSA mechanisms across biology and engineering confirm these predictions: mechanisms with lower accelerated mass generate higher acceleration (Ilton et al., 2018). Inherent trade-offs of muscles and springs lead to LaMSA mechanisms becoming less efficient at larger scales (Huxley, 1957; Rosario et al., 2016; Ilton et al., 2018; Sutton et al., 2019). Both frogs and mantis shrimp transition from spring-actuated movements in smaller species to muscle-actuated movements in larger species (Marsh, 1994; deVries et al., 2012). Interestingly, peak speeds of jumping insects occur at intermediate sizes, with lower values at both larger and smaller sizes (Ilton et al., 2018; Sutton et al., 2019). Examining performance at the lower end of LaMSA size helps establish whether smaller sizes limit spring-actuated mechanisms.

Mantis shrimp (Stomatopoda: Crustacea) offer a particularly amenable system for addressing the scaling of LaMSA within species. Adults use a LaMSA mechanism in their raptorial appendages (second thoracopods) to capture or process prey. Larval mantis shrimp raptorial appendages are similar in morphology to those of adults, but are an order of magnitude smaller in length (Haug et al., 2016; Haug and Haug, 2014; Feller et al., 2013; Wiethase et al., 2020; Gohar and Al-kholy, 1957; Morgan and Goy, 1987). Mantis shrimp species are commonly categorized as either smashers or spearers, although many other morphological shapes are present across the clade (Ahyong, 2001; Caldwell and Dingle, 1976). Adult smashers tend to be small and use hammer-shaped appendages to smash open hard-shelled prey, whereas some spearer species can grow to much larger adult body sizes and use appendages lined with large spines to capture free-swimming prey (deVries et al., 2012; McHenry et al., 2016). Smashers and spearers use a similar LaMSA mechanism to produce fast strikes, although the large spearing mantis shrimp *Lysiosquillina maculata* appears to primarily use muscles rather than springs to actuate strikes (Claverie and Patek, 2013; Anderson et al., 2014; Anderson and Patek, 2015; deVries et al., 2012). As for adults, larval mantis shrimp raptorial appendages are morphologically diverse. However, regardless of the adult morphotype, larval appendages do not exhibit the hammer shapes and spines found on the dactyls of adults (Fig. 1). Instead, larval dactyls are similar to the undifferentiated dactyls found in adults of the genus *Hemisquilla*, which use their appendages to knock limpets off rocks and are considered basal to the stomatopod clade (Van Der Wal et al., 2017; Porter et al., 2010; Claverie and Patek 2013).

To produce fast strikes, mantis shrimp use force-modified (long sarcomere length) extensor muscles in the merus segment of the raptorial appendage to contract and store elastic energy in the saddle and meral-V, which are exoskeletal regions of the merus that act as

¹Department of Biology, Duke University, Durham, NC 27708, USA. ²School of Life Sciences, University of Hawai'i at Mānoa, Honolulu, HI 96822, USA. ³Department of Ecology and Evolutionary Biology, University of California at Irvine, Irvine, CA 92697, USA. ⁴Department of Biological Sciences, Humboldt State University, Arcata, CA 95521, USA.

*Author for correspondence (jacob.harrison@duke.edu)

 J.S.H., 0000-0001-7752-6471; M.J.M., 0000-0001-5834-674X

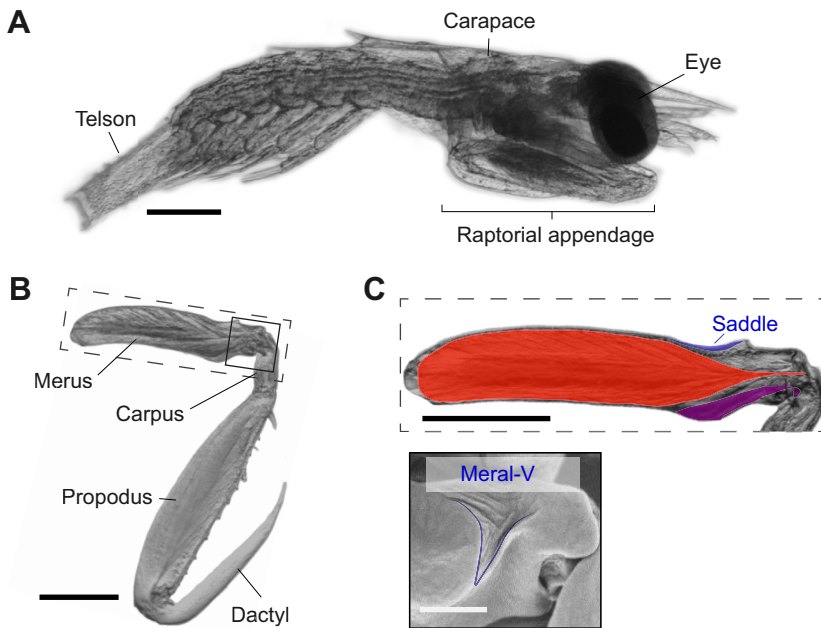


Fig. 1. Larval *Gonodactylaceus falcatus* use a latch-mediated spring actuation (LaMSA) mechanism in their raptorial appendages to produce fast strikes. (A) Lateral view of larval *G. falcatus* with anterior to the right of the page. (B) Raptorial appendages consist of four segments: merus, carpus, propodus and dactyl. (C) Larval merus morphology is similar to that of adults: large extensor muscles (red), a saddle and meral-V (blue), and flexor muscles attached to sclerites (modified apodemes; purple). These same components operate as the muscle, spring and latch for the adult LaMSA mechanism. Images in C show the outlined regions on the raptorial appendage in B. Black scale bars: 0.5 mm. White scale bar: 250 μ m.

an integrated elastic mechanism (Blanco and Patek, 2014; Patek et al., 2007; Rosario and Patek, 2015). Flexor muscles in the merus engage two sclerites (modified apodemes) which are braced against an invagination of the ventral merus exoskeleton and prevent rotation of the appendage (Burrows and Hoyle, 1972; Burrows, 1969). Shortly after the flexor muscles relax, the system unlatches, and the striking body (carpus, propodus and dactyl segments of the raptorial appendage; Fig. 1B) rotates anteriorly (Kagaya and Patek, 2016; Patek et al., 2007).

Comparisons of strike kinematics across mantis shrimp species reveal that smaller adult mantis shrimp produce higher rotational velocities and accelerations than larger adults (McHenry et al., 2016). This observation aligns with the predictions of LaMSA mathematical models (Ilton et al., 2018). Although the raptorial appendage morphology of larvae has been documented (Haug et al., 2016), the kinematics of their strikes has, to our knowledge, yet to be reported. It is therefore unknown whether larvae use LaMSA and, if they do, at which larval stage it develops. Here, we examined LaMSA kinematics and scaling across the substantial size range of larval and adult raptorial appendages. We reared larval Philippine mantis shrimp (*Gonodactylaceus falcatus*; Fig. 1A) and examined their raptorial appendage morphology using microscopy. Adult *G. falcatus* possess smashing raptorial appendages; however, during their larval stages, *G. falcatus* have undifferentiated appendages. In addition to rearing larvae from eggs, we collected *G. falcatus* larvae in the field and measured their raptorial appendage strikes using high-speed video. We compared their strike kinematics with an existing database of strike kinematics and morphology across adults of other mantis shrimp species and compiled a new dataset from the literature of similarly sized swimming and feeding larvae. We addressed the following questions. (1) Do larval mantis shrimp use a LaMSA mechanism and at which larval stage does this mechanism develop? (2) Given prior predictions of increasing acceleration at smaller sizes in LaMSA systems, how do the kinematics of mantis shrimp raptorial strikes scale from larvae to adults? (3) How do larval strike kinematics compare with the speed of their prey and the locomotion of organisms of similar scale?

MATERIALS AND METHODS

Specimen collection and maintenance

Eggs and freely swimming larvae of *Gonodactylaceus falcatus* (Forskål 1775) were collected on Oahu, HI, USA, in June 2019. We chose larval *G. falcatus* for this study because we could reliably collect them during our experiments. Larvae used for morphological imaging were raised for 28 days from a fertilized egg clutch that was collected by hand from an adult *G. falcatus* female at Wailupe Beach Park, Oahu, HI, USA. Eggs were shipped to Duke University and hatched en route. Hatched larvae were distributed between two 2 l plastic containers which were filled with synthetic saltwater ($\sim 27^{\circ}\text{C}$, salinity ~ 30 ppt) and cleaned daily. Cleaning consisted of a 50% water change and removal of any waste, molts or dead larvae. The containers were placed on a variable speed shaker table to keep water moving and to simulate their natural environment. Once they began feeding, during the fourth larval stage, larvae were fed 1–2 day old *Artemia* nauplii (~ 25 – 30 nauplii ml^{-1}). To determine the duration of each larval stage, 3–5 live *G. falcatus* larvae were fixed daily in 4% glutaraldehyde with 0.2 mol l^{-1} PBS and 12% sucrose. To compare morphology across larval stages, we collected digital images of the lateral side of the body and raptorial appendages (2560×1920 pixel resolution; DFC 450 C camera; model 165M FC microscope; Leica Microsystems Inc., Buffalo Grove, IL, USA). Each image was embedded with a digital scale bar calibrated using a 0.02 mm stage micrometer.

Larvae that were used for measuring strike kinematics were collected by suspending underwater lights off boat docks near adult *G. falcatus* habitats. Mantis shrimp larvae were identified using diagnostic morphological characteristics (M.L.P., unpublished data). Only larvae identified morphologically as *G. falcatus* were used in kinematic analyses. The larvae were transported to the University of Hawai'i at Mānoa to film their strikes. During mantis shrimp development, larvae transition from a propelagic phase when they remain inside the adult's burrow, to a pelagic phase when they swim freely in the water column. Larvae are only positively phototactic during their pelagic stages (starting at stage 4 in *G. falcatus*). Because larvae were attracted to underwater lights, all

G. falcatus larvae used for measuring strike kinematics were in their fourth, fifth or sixth larval stages.

After high-speed imaging was completed, the anterior halves of individuals were fixed in a 4% glutaraldehyde, 0.1 mol l⁻¹ sodium cacodylate with 0.35 mol l⁻¹ sucrose solution and shipped to Duke University. The posterior halves of individuals were fixed in 100% ethanol to confirm species identification using established genetic barcoding methods for larval mantis shrimp (Palcanda et al., 2020). The posterior halves of individuals were extracted using a DNeasy Blood and Tissue kit (Qiagen); lysis was performed overnight at 56°C with gentle agitation, and DNA was eluted from each column twice into a total volume of 100 µl. DNA extractions from each individual were quantified using the DNA HS kit with a Qubit fluorometer, followed by PCR and sequencing using primers for the 18S rRNA gene (primers a0.7 and bi – see Porter et al., 2010). All PCR amplifications used 2× Quick Load Taq (NEB) with the following thermocycling conditions: initial denaturation of 94°C for 30 s; 50 cycles of 94°C for 20 s, 46°C for 10 s, 72°C for 60 s; final extension at 72°C for 7 min. The 18S PCRs used ratios of 8 ng DNA:0.1 mmol l⁻¹ primer, and a total reaction volume of 10 µl. All products were run on a 0.8% agarose gel at 100 V for 20 min. Successful amplifications were cleaned using 1.0–1.2 µl ExoSAP (1×) and sequenced at the Advanced Studies in Genomics, Proteomics and Bioinformatics core at the University of Hawai'i. Species identity was determined using BLAST searches in NCBI and confirmed by phylogenetic analyses with 18S sequence databases from Hawaiian mantis shrimp species (M.L.P., unpublished data). PCR amplifications of the 18S gene were successful for only seven of the 12 individuals used in kinematic experiments (Table 1). All sequences were deposited in GenBank (accession numbers: MW391490–MW391496).

LaMSA mechanism

At the fourth larval stage, the reared larvae began moving their raptorial appendages and feeding on *Artemia* nauplii. Live fourth-stage larvae ($n=2$) were placed between a glass slide and coverslip and filmed under the microscope using a high-speed video camera (Movie 1; model 165M FC stereomicroscope, Leica Microsystems Inc.; 703×688 pixel resolution, 20,000 frames s⁻¹, FastCAM SA-Z, Photron, San Diego, CA, USA). The exoskeleton of larval raptorial appendages is largely transparent, and thus we were able to visualize external movements of cuticle and internal movements of muscles prior to and during raptorial appendage strikes. We captured high-speed video of two full sequences of elastic loading, latch release and striking body rotation from two individuals. For one of the LaMSA sequences, we tracked two points on the lateral extensor muscle, two points on the saddle and two points on the lateral flexor muscle over the duration of the strike to approximate the length change for each element during the strike (MtrackJ, v1.5.1; Meijering et al., 2012; ImageJ v.2.0.0, National Institutes of Health, Bethesda, MD, USA; Schneider et al., 2012). Tracked points were placed at the origin and insertion for both the lateral extensor and lateral flexor muscles as well as the proximal and distal tips of the saddle (Fig. S1). These elements represent only part of the mantis shrimp LaMSA mechanism. Because of the transparency of the tissue and orientation of the appendage, we were unable to visualize the meral-V, apodeme, medial extensor muscle and medial flexor muscle during the strike. We compared the timing and duration of length changes of the extensor muscle, flexor muscle and saddle with the rotation of the striking body. To calculate strike rotation, we tracked two points along the merus and two points along the propodus. Positional data from tracked points were

Table 1. Strike kinematics of larval *Gonodactylaceus falcatus*

Individual	Species	No. of strikes	Striking body length (mm)	Accelerated mass (mg)	Strike duration ($\times 10^{-3}$ s)	Angular displacement (rad)	Angular velocity (rad s ⁻¹)	Angular acceleration ($\times 10^5$ rad s ⁻²)	Linear speed (m s ⁻¹)	Linear acceleration ($\times 10^5$ m s ⁻²)	Reynolds no.
1		1	1.2		10.00	0.90	188.9	2.473	0.222	2.90	310
2	<i>G. falcatus</i>	2	1.2		3.9±1.5	1.13±0.41	518.8±170.7	7.401±0.587	0.614±0.202	8.76±0.69	850±280
3	<i>G. falcatus</i>	2	1.3		6.8±2.45	1.15	295.4±144.7	2.194±1.403	0.388±0.190	2.88±1.84	600±290
4	<i>G. falcatus</i>	1	1.2		4.90	1.31	553.5	13.173	0.681	16.22	990
5		2	1.4	0.006	23.15±9.69	1.27±0.19	73.3±22.1	0.429±0.231	0.100±0.030	0.58±0.31	160±50
6		1	1.4	0.017	4.80	0.81	34.6	2.455	0.480	3.45	790
7		6	1.4	0.013	7.85±3.42	1.01±0.33	294.7±247.3	3.534±2.953	0.405±0.340	4.85±4.05	650±550
8		1	1.4	0.010	5.80	0.58	193.1	5.816	0.260	7.85	410
9	<i>G. falcatus</i>	1	1.4	0.010	2.55	0.64	291.2	3.215	0.411	4.54	680
10	<i>G. falcatus</i>	1	1.4	0.010	6.30	0.92	275.9	2.222	0.380	3.06	613
11	<i>G. falcatus</i>	1	1.4	0.013	13.55	1.23	235.6	3.273	0.325	4.51	530
12	<i>G. falcatus</i>	6	1.4	0.012	12.63±9.56	1.05±0.20	250.3±142.8	3.422±3.123	0.350±0.199	4.78±4.36	570±330
Overall mean±s.d.			1.3±0.1	0.011±0.003	8.52±5.7	1.0±0.24	292.7±133.3	4.134±3.363	0.385±0.159	5.37±4.06	596±230

Data are presented as means±s.d. for each individual. Species confirmation (where indicated) was obtained from 18S RNA sequences.

converted into length changes and angular displacement using custom-written R code (v1.1.456, RStudio, Boston, MA, USA; <http://www.R-project.org/>; available from Dryad, doi:10.5061/dryad.3n5tb2rf7).

To determine whether larvae at the fourth larval stage have a meral-V, we used scanning electron microscopy. Three fourth-stage larvae were transferred stepwise to 100% ethanol, and summarily chemically dried using hexamethyldisilazane (HMDS). Dried larvae were gold sputter coated (Desk IV, Denton Vacuum, Moorestown, NJ, USA) and imaged using a scanning electron microscope (Hitachi TM3030Plus Tabletop SEM, Hitachi Ltd, Tokyo, Japan).

Strike kinematics

Larval strikes ($n=25$ strikes across 12 individuals, 1–6 strikes per individual) were visualized using high-speed imaging (1024×1024 pixel resolution, K2 Video Lens, Edmund Optics, Barrington, NJ, USA; 20,000 frames s^{-1} , FastCAM SA-Z, Photron). Because of their small size, and in order to position the larvae within the field of view of the camera, we attached each larva to a custom-designed platform (Fig. S1A). Each larva was removed from its container, quickly air dried, and a toothpick was affixed to its carapace using cyanoacrylate glue. Gluing toothpicks to the shield (carapace) restrained the larva's body while still allowing their raptorial appendages to strike. When the glue was sufficiently dry, the toothpick and larva were attached to the platform, submerged in fresh seawater, and illuminated for high-speed imaging (75 W LED, Varsa Nila, Inc., Altadena, CA, USA). Micromanipulators were used to bring the larva into focus. Each larva was oriented laterally to the camera. Defensive strikes were elicited by agitating the larva with a toothpick (Movie 2).

We performed a kinematic analysis of the strikes. From each recording, we manually tracked four points along the raptorial appendage: two points on the propodus segment and two points on the merus segment (Fig. S2; MtrackJ plugin, v1.5.1, Meijering et al., 2012; ImageJ v.2.0.0, Schneider et al., 2012). Point tracking began just before the onset of propodus rotation and ended when the propodus reached its maximal extension. A sixth-order polynomial model was fitted to the rotational data using custom-written R scripts, and the first and second derivatives (velocity and acceleration) were calculated from the fitted model (R code available from Dryad, doi:10.5061/dryad.3n5tb2rf7). Videos were calibrated using a millimeter-scale ruler filmed in the plane of focus. To increase the precision of the videos, the ruler was re-calibrated to 0.1 mm using a 0.02 mm scale under a microscope [KR-814 (1×3) stage micrometer, Klarmann Rulings, Inc., Litchfield, NH, USA]. Angular kinematics were converted to linear kinematics (e.g. speed and linear acceleration) by multiplying the peak angular kinematics in radians by the length of the striking body. We measured the striking body length, defined as the length from the propodus–dactyl joint to the insertion point of the lateral extensor muscle on the dorsal surface of the carpus, for each larvae from high-speed videos. To calculate digitizing error, one random strike was digitized 10 times. We found that the standard error of the mean from digitizing constituted 0.3% of the reported rotation measurement, 0.5% of the velocity measurements and 1.1% of the acceleration measurements (Fig. S3). The scaling of angular kinematics (velocity and acceleration) was analyzed in terms of striking body length, strike duration and strike angular displacement using ordinary least squares (OLS) regressions in R (v1.1.456, RStudio; <http://www.R-project.org/>).

After filming, each raptorial appendage was surgically removed, imaged (same microscope setup as above) and weighed using a

microbalance scale (resolution: 1 μg ; XPE56 Mettler Toledo, Pleasant Prairie, WI, USA). This process was repeated for the striking body (dactyl, propodus and carpus) by removing the merus from the rest of the appendage. Each mass measurement was repeated 3 times. During the fixation process, four of the 12 larvae became disarticulated; therefore, we only report striking body mass for eight individuals.

Kinematic comparisons

We compared the larval strike kinematics with a previously compiled dataset of adult mantis shrimp strike kinematics that were recalculated from the original research papers (McHenry et al., 2016). The dataset in McHenry et al. (2016) was based on the maximum kinematics (angular and linear velocity and acceleration) originally reported from adult *Odontodactylus scyllarus* (Patek et al., 2007), *Lysiosquillina maculata* and *Alachosquilla vicina* (deVries et al., 2012), *Gonodactylus smithii* (Cox et al., 2014), *Neogonodactylus bredini* (Kagaya and Patek, 2016) and *Coronis scolopendra* (McHenry et al., 2016). Kinematics from adult and larval mantis shrimp strikes were compared in terms of striking body length.

Larval *G. falcatus* strike speeds were compared with the swimming and feeding speeds (mouth opening speed) of other small pelagic organisms. We gathered total body length and maximum recorded speeds from the literature on larval fish (Fisher et al., 2005; Bellwood and Fisher, 2001; Clark et al., 2005; China et al., 2017), larval crustaceans (Williams, 1994; Walker, 2004), larval bryozoans (Wendt, 2000) and larval tunicates (McHenry et al., 2003). We compared these data with our dataset of larval mantis shrimp strike kinematics and total body size. We measured total length of the fourth-stage larval mantis shrimp using digital images from a lateral view of each larva; total length was defined as the distance from the anterior tip of the carapace (shield) to the posterior tip of the telson at the midline.

RESULTS

Larval development

We performed behavioral and morphological observations while raising larval *G. falcatus* through all six larval stages (Fig. 2). During the first two stages, larvae were negatively phototactic, preferring to stay aggregated together at the bottom of their tank. At the third stage, larvae began swimming independently, but remained negatively phototactic. During the first three stages, larvae still possessed yolk sacs and the raptorial appendage segments had not yet differentiated (Fig. 2). At the fourth larval stage (days 9–14), larvae exhibited a behavioral and morphological transition. Larvae began striking and ‘waving’ their raptorial appendages as they swam through the water; at this stage, larvae began feeding on *Artemia* nauplii (determined by orange coloration of the gut) and fully lost their yolk sac. Larvae in the fifth and sixth stages were larger than those in the fourth stage, but had similar body and raptorial appendage shapes. Sixth-stage larvae had larger spines lining the propodus than in the previous stages.

LaMSA mechanism

At the fourth larval stage, *G. falcatus* raptorial appendages were fully differentiated into the merus, carpus, propodus and dactyl segments. The saddle and meral-V were present on the merus exoskeleton (Fig. 1). In the merus, large extensor muscles inserted on the carpus and two flexor muscles connected to internal sclerites.

The sequential activation of the LaMSA mechanism was determined through digital image analysis of the timing of length

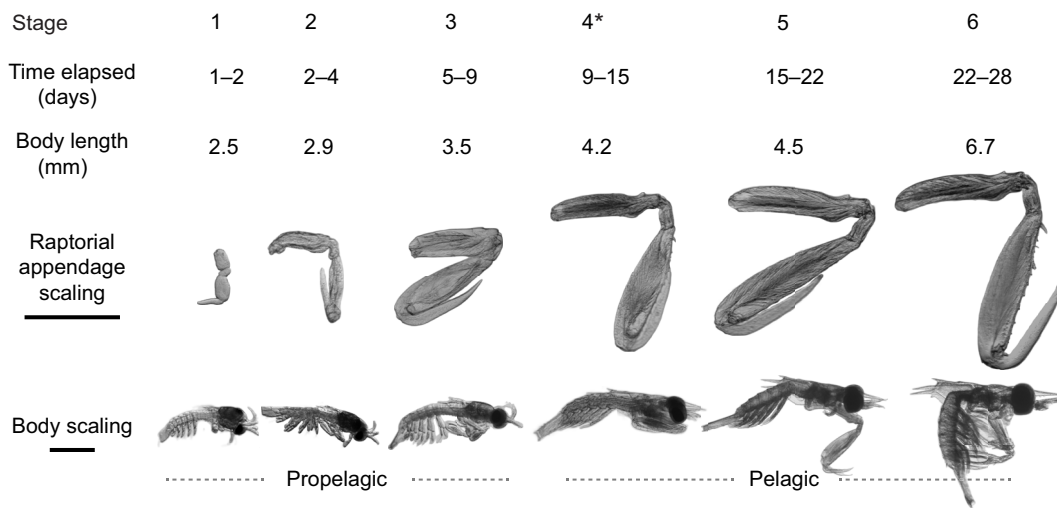


Fig. 2. Larval *G. falcatus* develop raptorial appendages in their early larval stages and possess a fully functional LaMSA mechanism by the fourth larval stage. During stage 4 (asterisk), larvae begin feeding and enter the pelagic zone (Shanhogue, 1978) and also transition morphologically to using a LaMSA mechanism. Time elapsed represents the number of days from hatching (day 0) to the end of our study (day 28). Body length was measured from the anterior tip of the shield to the posterior end of the telson at the midline. Scale bars: 1 mm.

changes of the lateral extensor muscle and lateral flexor muscle, and appendage rotation of one strike (Fig. S1). The largely transparent raptorial appendages enabled visualization of conformational changes of the internal morphology, including contraction and relaxation of the lateral flexor and lateral extensor muscles. During preparation for the strike, the extensor muscle shortened, the saddle changed length, and the striking body did not rotate (Fig. S1). When the flexor muscle relaxed (lengthened), the lateral sclerite visibly slid along the ventral surface of the merus, thereby unlatching the LaMSA mechanism and allowing the striking body to rotate (Fig. S1, Movie 1). It should be noted that this analysis was performed on a relatively fast strike (679.9 rad s^{-1} , $12.103 \times 10^5 \text{ rad s}^{-2}$) compared with our complete dataset (Table 1), possibly as a result of the different experimental setup during filming.

Strike kinematics

Striking behavior was similar to previous reports in adult mantis shrimp. In preparation for the strike, the dactyl and propodus were flexed toward the merus. The dactyl was then opened until it was roughly perpendicular to the propodus. The appendage was held in this position for ~ 30 ms, until the strike initiated and the striking body (carpus, propodus and dactyl) rotated towards the target. The average peak angular velocity from larval strikes was 292.7 rad s^{-1} ($n=25$ strikes across 12 individuals, 1–6 strikes per individual). Average strike speed was 0.385 m s^{-1} . Summary statistics for each individual are presented in Table 1.

Peak angular velocity and peak angular acceleration were not statistically correlated with striking body length (1.2–1.4 mm) or maximum rotation (0.58–1.60 rad). Angular acceleration was not significantly correlated with strike duration (2.55–23.15 ms). Peak angular velocity was negatively correlated with strike duration (slope= -1.5×10^4 , $t=-2.92$, d.f.=10, $P=0.015$).

Kinematic comparisons

Strike kinematics across mantis shrimp species is associated with raptorial appendage size (Fig. 3). Larval *G. falcatus* achieved angular velocities and accelerations that were in the same range as for smaller adult spearing mantis shrimp, such as *C. scolopendra*. Larval angular kinematics were lower than for the adult smashing mantis shrimp, but

greater than for the largest mantis shrimp species, *L. maculata* (Fig. 3A,B). However, the linear speed of larval strikes was an order of magnitude lower than for adult mantis shrimp (Fig. 3C).

Strikes by mantis shrimp larvae were 5–10 times faster than the speed of similarly sized larval fish and crustaceans (Fig. 4). During their development in the laboratory, *G. falcatus* larvae fed on larval *Artemia* nauplii. Their strikes were over two orders of magnitude faster than previously reported peak swimming speeds of first- and second-stage *Artemia* nauplii (Williams, 1994).

DISCUSSION

Larval *G. falcatus* exhibit LaMSA in their raptorial appendages (Fig. 1). In one of the spring-actuated strikes we analyzed, large extensor muscles deformed the merus exoskeleton while the flexor muscles and sclerites prevented rotation of the striking body. When the flexor muscles relaxed, the sclerites disengaged, and the striking body rotated distally (Fig. S1, Movie 1). This sequence of events is consistent with the presence of a LaMSA mechanism, specifically the storage and delivery of elastic energy via latch mediation. The larval LaMSA morphology emerges at the fourth larval stage (~ 9 –14 days old), when larvae in the wild first enter the pelagic zone and begin feeding (Fig. 2). Larvae strike with angular velocities and accelerations that are similar to those of adult spearing mantis shrimp. However, the peak linear speed of the larval strike is over an order of magnitude slower than for adults (Fig. 3; McHenry et al., 2016). Larval strikes were 5–10 times faster than the reported swimming speeds of similarly sized organisms and two orders of magnitude faster than the *Artemia* nauplii the larvae fed on during our experiments (Fig. 4). Below, we examine these results in the context of adult mantis shrimp morphology and kinematics and discuss the implications of scaling and development of LaMSA mechanisms in biology.

Larval LaMSA morphology is similar to that of adult mantis shrimp. At the fourth larval stage, *G. falcatus* have large extensor muscles, a saddle and meral-V, and flexor muscles attached to internal sclerites (Fig. 1). We provide an analysis of a strike sequence in Fig. S1, and include a general description here. In the larval strike, sclerites embedded in the apodemes of the flexor muscles prevent the rotation of the striking body when the flexor

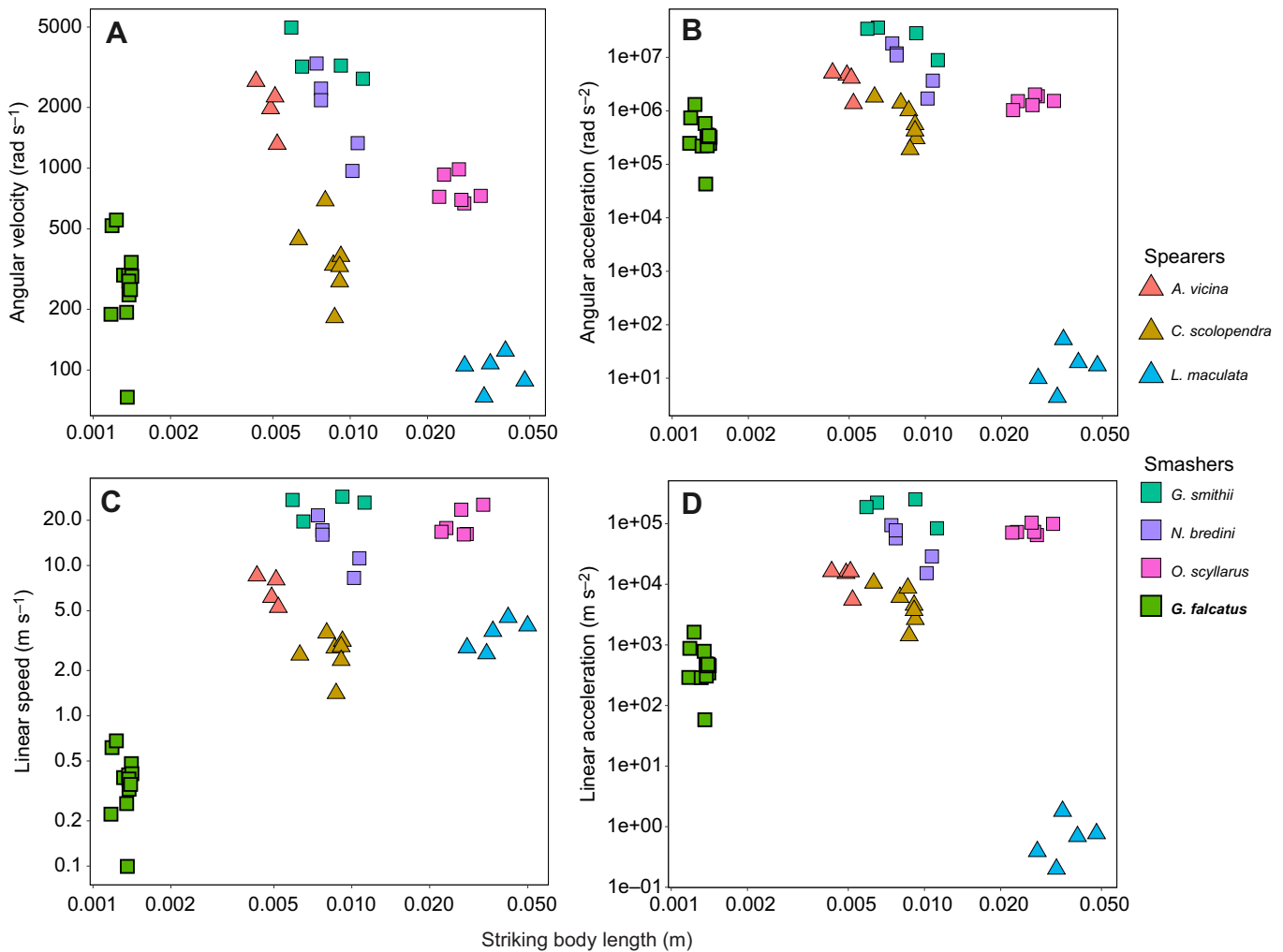


Fig. 3. Larval *G. falcatus* generate angular strike kinematics that are comparable with those of adults, even though adult raptorial appendages are an order of magnitude longer than in larvae. Larval *G. falcatus* (green squares) angular velocity (A) and angular acceleration (B) are similar to those of adult strikes in other species (*Alachosquilla vicina*, *Coronis scolopendra*, *Lysiosquilla maculata*, *Gonodactylus smithii*, *Neogonodactylus bredini* and *Odontodactylus scyllarus*). The linear speed (C) of larval strikes is lower than for adult strikes. Linear acceleration (D) of larval strikes is lower than that of most adults strikes, but greater than that of the largest spearing adults ($N=12$ individual larvae; 1–6 strikes per individual). The adult mantis shrimp kinematics represent maximum values from each individual within each species (data from McHenry et al., 2016).

muscles are contracted. As the extensor muscles in the merus contract, the saddle and merus exoskeleton deform. When the flexor muscles relax, the paired sclerites slide distally, allowing the striking body to rotate forward and the saddle to recoil (Fig. S1). In the adult LaMSA mechanism, the saddle and meral-V comprise the elastic mechanism (Rosario and Patek, 2015; Zack et al., 2009; Patek et al., 2004) and release of elastic energy is mediated by the paired flexor muscles and internal sclerites (Burrows, 1969; Patek et al., 2007; Kagaya and Patek, 2016). The similarities between the larval and adult LaMSA sequences suggest that the saddle stores and releases elastic energy in the larval raptorial appendage as well. The dynamics of this tiny elastic mechanism, specifically how it delivers energy to the larval rotation at these scales, is an exciting future direction for this research.

Development of the LaMSA morphology in *G. falcatus* occurs as larvae transition to the pelagic zone, which coincides with the loss of the yolk sac and subsequent onset of feeding. Prior studies of larval *G. falcatus* development showed that when larvae transition to their fourth stage, they exhaust their yolk sac and transition to the pelagic zone (Gohar and Al-Kholly, 1957; Shanbhogue, 1978).

Here, we support those findings and further show that this pelagic transition includes the development of LaMSA morphology. Developmental series have been examined for several mantis shrimp families: Gonodactylidae (Morgan and Goy, 1987; Provenzano and Manning, 1978), Squillidae (Diaz, 1998; Hamano and Matsuura, 1987; Morgan and Provenzano, 1979; Pyne, 1972) and Tetrasquillidae (Greenwood and Williams, 1984). Regardless of the family, all stomatopod species transition from a propelagic stage to a pelagic stage at some point during their development and morphological drawings of these transitions show large, fully developed raptorial appendages that emerge at, or before, this transition (Pyne, 1972; Morgan and Goy, 1987; Hamano and Matsuura, 1987). The presence of larval raptorial appendages across the phylogeny of mantis shrimp suggests that *G. falcatus* is not unique among mantis shrimp and that other larvae likely possess a LaMSA mechanism. However, larval mantis shrimp size and shape are as diverse as those of their adult counterparts (Haug et al., 2016). Further research on the diversity of LaMSA mechanisms within mantis shrimp larvae will be important to establish whether spring actuation is found during this life history stage in other mantis shrimp species.

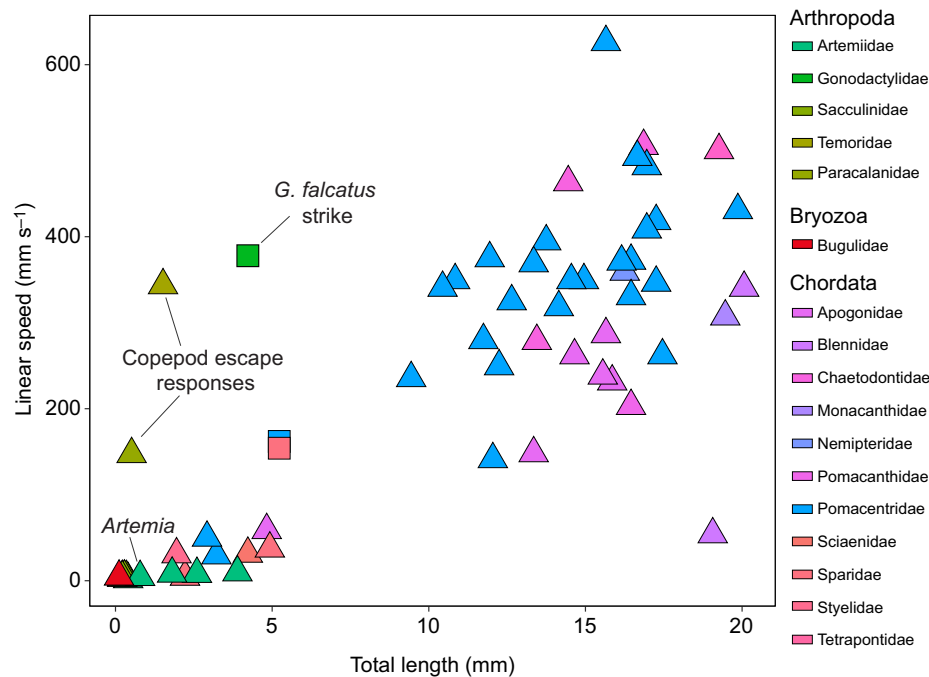


Fig. 4. Larval *G. falcatus* strike speeds are over two orders of magnitude faster than the prey (*Artemia* sp.) speed, whereas the swimming speeds of larger larvae from other species rival the strike speeds of larval mantis shrimp. Each point represents the speed of a larval pelagic organism ($n=54$ species), including feeding (squares) and swimming (triangles). Each color represents a different taxonomic family-level designation across fish and crustaceans. Data and sources are listed in Table S1.

We did not find a strong scaling relationship between strike kinematics and size within larvae; however, the size range of their striking body (1.2–1.4 mm) through these stages of development is so small that differences due to scaling may not be detectable or relevant. Strike kinematics have not yet been measured in adult *G. falcatus*. Across species, however, smaller adult mantis shrimp produce higher angular velocities and accelerations than larger adults (McHenry et al., 2016), and adult smashing mantis shrimp species produce faster kinematics than similarly sized spearing mantis shrimp species (McHenry et al., 2016). Adult *G. falcatus* are a relatively small smashing species, similar in body size and ecological niche to *N. bredini* and *G. smithii*, which have the fastest strike kinematics measured within mantis shrimp (Kagaya and Patek, 2016; Cox et al., 2014). Larval *G. falcatus* strike angular velocity and acceleration are similar to those of *C. scolopendra*, one of the smaller adult spearing mantis shrimp species (Fig. 3A,B; McHenry et al., 2016). Angular velocity, angular acceleration and linear acceleration are all highest in the intermediate size range across mantis shrimp species. The linear speed of the larval *G. falcatus* strike is an order of magnitude slower than that of adults (Fig. 3C; McHenry et al., 2016; deVries et al., 2012). By this metric, the larval kinematics are impressive for a small pelagic organism, but less impressive when compared with those of small adult mantis shrimp. There are several potential reasons why larvae strike more slowly than adults, such as scaling limitations due to their biomechanics (e.g. fluid interactions and LaMSA) or their behavioral ecology in a pelagic environment.

Like many small planktonic organisms, mantis shrimp larvae primarily operate in low to intermediate Reynolds numbers (Re ; Daniel et al., 1992; McHenry et al., 2003). The Re is dependent on the organism's size and speed, and quantifies the relative viscous and inertial fluid forces (Vogel, 1981). The peak Re of the larval *G. falcatus* strikes ranges between 123 and 1649, which places larvae in an intermediate Re regime. Given that these appendages operate at intermediate Re , they likely experience both viscous and inertial fluid forces such as skin friction, form force and the acceleration reaction (McHenry et al., 2003), all of which

decelerate movement and would potentially limit the kinematics of larval strikes.

Another limit to larval strike kinematics likely arises from the scaling of muscle–spring systems. Smaller muscles produce lower force than larger muscles and smaller springs deform smaller distances than larger springs. If the spring maintains its stiffness across size, the muscle would be challenged to deform the spring at small scales, as a result of the scale dependence of muscle force. If spring stiffness were instead lower in a smaller animal, then the system would have less capacity for elastic energy storage (Rosario, et al., 2016). Additionally, if spring stiffness were invariant with size, then the likelihood of fracture or breakage of the spring would be greater in a smaller structure (Ilton et al., 2018). Smaller organisms might exhibit lower spring stiffness such that the system can be loaded with less risk of failure, yet this ultimately limits stored energy and thus reduces the kinematic output. Further work on the ontogeny of spring stiffness in the mantis shrimp system, as well as other LaMSA mechanisms, will illuminate how small, ultrafast movements have evolved to navigate these muscle–spring tradeoffs.

Adult mantis shrimp LaMSA mechanisms have multiple uses, including prey capture (deVries et al., 2012), prey processing (Crane et al., 2018), and intraspecific or interspecific competition (Caldwell and Dingle, 1976). Adult mantis shrimp vary the kinematics of their strikes depending on the behavioral context (Green et al., 2019). Early work on larval stomatopod morphology and development suggested that the raptorial appendages are used for prey capture (Morgan and Goy, 1987). Given that the appendages are fully developed when larval *G. falcatus* begin feeding, larvae likely use raptorial appendage strikes for prey capture or prey processing when in the wild, even though our study exclusively examined defensive strikes. Using spring energy to enhance mechanical power output and increase strike speed relative to a muscle-driven strike may enable the larvae to impale prey, rather than pushing the prey further away as a result of fluid boundary layers. Because of the need to mount the animals under a microscope to image these movements, we were unable to film

natural feeding strikes and behavior using high-speed imaging. Further investigations of freely moving and feeding animals, coupled with fluid dynamic modeling, are necessary to establish the role of fluid interactions on the ability of these larvae to impact and capture planktonic prey.

While larval strikes have a slower linear speed than the fastest adult mantis shrimp, they are still impressive for a 4 mm long pelagic organism. Larval *G. falcatus* achieve strike speeds that are 5–10 times faster than the peak swimming speeds of similarly sized organisms, and over 150 times faster than the *Artemia* nauplii that the larvae fed on in our experiments (Fig. 4; Table S1). At the fourth larval stage, lab-raised *G. falcatus* fed on *Artemia* nauplii as well as other larval *G. falcatus* (J.S.H., personal observation). Although larval *G. falcatus* do not naturally feed on *Artemia*, they are able to capture and feed on prey of similar size. Other planktivores, such as larval fish, are often unsuccessful during feeding attempts because of fluid boundary layers (China et al., 2017) or prey escape behavior (Robinson et al., 2019). Based on these comparative data and their *Re* regime, larval mantis shrimp strikes may be sufficiently fast to capture planktonic prey (Fig. 4). Further research should incorporate additional data on the escape speeds of small pelagic organisms that might exceed the swimming and feeding speeds reported here. For example, copepod rapid escape responses can reach similar speeds to larval mantis shrimp strikes (of the order of 10^2 mm s^{-1} ; Fig. 4; Bradley et al., 2013). In addition, it should be noted that most prior studies on pelagic larval swimming used video frame rates much lower than those used in this study, and therefore may have underestimated the actual swimming speeds at these scales. Adult smashing and spearing mantis shrimp both have wide diets that include hard-shelled and soft-bodied prey, though smashers consume a greater proportion of hard-shelled prey and spearers prefer soft-bodied evasive prey (deVries, 2017). The relationship between mantis shrimp strike kinematics and the swimming speeds of their potential prey is an interesting area for future study.

Larval mantis shrimp offer a novel system not only to resolve ongoing questions about the mantis shrimp LaMSA mechanism but also to address fundamental questions about spring–latch dynamics and the scaling of elastic mechanisms in biology. In adult mantis shrimp, the four-bar linkage mechanism in the raptorial appendage responsible for transmission of elastic energy into rotation of the striking body may also act as a geometric latch – a latch that restricts behavior based on geometric configuration rather than a physical obstruction (Patek, 2019; Longo et al., 2019). The transparency of the larval merus enables visualization of energy transfer between elastic elements and the role of the internal sclerites. The timing of sclerite release in relation to the onset of rotation may ultimately reveal whether the linkage mechanism acts as a secondary latch. This transparency also allows measurements of latch morphology and the kinematics of latch disengagement is key for estimating energetic losses during latch release.

Larval mantis shrimp may be one of the smallest known repeatable LaMSA mechanisms in biology (Longo et al., 2019; Longo et al., 2021; Nüchter et al., 2006; Sakes et al., 2016). An emerging boundary of small, fast and repeatable biological LaMSA systems includes snapping amphipods (Longo et al., 2021), jumping nematodes (Campbell and Kaya, 1999), trap-jaw ants (Larabee et al., 2018) and termites (Seid et al., 2008). LaMSA systems that are smaller and have higher accelerations self-destruct, such as in nematocysts (Nüchter et al., 2006). Further research on these small repeatable mechanisms will help biologists and materials scientists understand the scaling and material limits to elastic energy storage.

Conclusions

This study establishes the development and kinematics of the larval mantis shrimp raptorial appendage strike. These strike kinematics are comparable with the strikes of adult mantis shrimp which have raptorial appendages that are one to two orders of magnitude longer than the larval appendages. The morphology needed to store elastic energy emerges at the larval stage when feeding begins. Their LaMSA mechanism likely enables them to achieve strike speeds far exceeding the escape speeds of their prey and to transition out of the viscous realm and into the inertial realm such that they can impact and impale their tiny prey (Nüchter et al., 2006; Hamlet et al., 2020). These findings yield insights into the scaling and development of LaMSA and establish a novel transparent and repeatable LaMSA system to explore the dynamics of elastic energy storage and release.

Acknowledgements

Thanks to M. Steck and M. Johnson-Griggs for help generating sequence barcoding data. Thanks to S. Palecandra, M. McDonald, A. Loomis, L. Carly and E. Sonenshine for their help collecting specimens. Thanks to S. Longo, C. Reynaga, J. Jorge, J. Dinh and W. Ray for comments on the manuscript. Special thanks to G. Budziszewski for her support.

Competing interests

The authors declare no competing or financial interests.

Author contributions

Conceptualization: M.L.P., M.J.M., H.E.R., S.N.P.; Methodology: J.S.H., M.L.P., M.J.M., H.E.R., S.N.P.; Formal analysis: J.S.H., M.L.P.; Investigation: J.S.H., M.L.P.; Resources: J.S.H., M.L.P., S.N.P.; Data curation: J.S.H.; Writing - original draft: J.S.H., S.N.P.; Writing - review & editing: J.S.H., M.L.P., M.J.M., H.E.R., S.N.P.; Visualization: J.S.H.; Supervision: M.L.P., S.N.P.; Project administration: S.N.P.; Funding acquisition: J.S.H., M.L.P., S.N.P.

Funding

Funding was provided by a Company of Biologists Travelling Fellowship to J.S.H. (JEBTF181185) and a National Science Foundation grant to S.N.P. (IOS 1439850). This material is based upon work supported by, or in part by, the U.S. Army Research Laboratory and the U.S. Army Research Office under contract/grant number W911NF-15-1-058, awarded to S.N.P. M.J.M. was supported by the Office of Naval Research (N00014-19-1-2035 and N00014-17-1-2062) and a National Science Foundation grant (IOS-2034043). M.L.P. was partially supported by the National Science Foundation (EPSCoR RII 1738567) and the University of Hawai'i at Mānoa.

Data availability

All datasets and computer coding are available from the Dryad digital repository (Harrison et al., 2020): doi:10.5061/dryad.3n5tb2r7f. 18S rRNA gene sequences are available from GenBank (accession numbers: MW391490–MW391496).

Supplementary information

Supplementary information available online at <https://jeb.biologists.org/lookup/doi/10.1242/jeb.235465.supplemental>

References

- Ahyong, S. T. (2001). *Revision of the Australian Stomatopod Crustacea*. Sydney, Australia: Australian Museum.
- Anderson, P. S. L. and Patek, S. N. (2015). Mechanical sensitivity reveals evolutionary dynamics of mechanical systems. *Proc. R. Soc. B* **282**, 20143088. doi:10.1098/rspb.2014.3088
- Anderson, P. S. L., Claverie, T. and Patek, S. N. (2014). Levers and linkages: mechanical trade-offs in a power-amplified system. *Evolution* **68**, 1919–1933. doi:10.1111/evo.12407
- Bellwood, D. R. and Fisher, R. (2001). Relative swimming speeds in reef fish larvae. *Mar. Ecol. Prog. Ser.* **211**, 299–303. doi:10.3354/meps211299
- Blanco, M. M. and Patek, S. N. (2014). Muscle trade-offs in a power-amplified prey capture system. *Evolution* **68**, 1399–1414. doi:10.1111/evo.12365
- Bradley, C. J., Strickler, J. R., Buskey, E. J. and Lenz, P. H. (2013). Swimming and escape behavior in two species of calanoid copepods from nauplius to adult. *J. Plankton Res.* **35**, 49–65. doi:10.1093/plankt/fbs088

- Burrows, M.** (1969). The mechanics and neural control of the prey capture strike in the mantid shrimps *Squilla* and *Hemisquilla*. *Z. Vergl. Physiol.* **62**, 361-381. doi:10.1007/BF00299261
- Burrows, M. and Hoyle, G.** (1972). Neuromuscular physiology of the strike mechanism of the mantis shrimp, *Hemisquilla*. *J. Exp. Zool.* **179**, 379-393. doi:10.1002/jez.1401790309
- Caldwell, R. L. and Dingle, H.** (1976). Stomatopods. *Sci. Am.* **234**, 80-89. doi:10.1038/scientificamerican0176-80
- Campbell, J. F. and Kaya, H. K.** (1999). Mechanism, kinematic performance, and fitness consequences of jumping behavior in entomopathogenic nematodes (*Steinernema* spp.). *Can. J. Zool.* **77**, 1947-1955. doi:10.1139/z99-178
- China, V., Levy, L., Liberzon, A., Elmaliach, T. and Holzman, R.** (2017). Hydrodynamic regime determines the feeding success of larval fish through the modulation of strike kinematics. *Proc. R. Soc. B* **284**, 20170235. doi:10.1098/rspb.2017.0235
- Clark, D. L., Leis, J. M., Hay, A. C. and Trnski, T.** (2005). Swimming ontogeny of larvae of four temperate marine fishes. *Mar. Ecol. Prog. Ser.* **292**, 287-300. doi:10.3354/meps292287
- Claverie, T. and Patek, S. N.** (2013). Modularity and rates of evolutionary change in a power-amplified prey capture system. *Evolution* **67**, 3191-3207. doi:10.1111/evo.12185
- Cox, S. M., Schmidt, D., Modarres-Sadeghi, Y. and Patek, S. N.** (2014). A physical model of the extreme mantis shrimp strike: kinematics and cavitation of Ninjabot. *Bioinspir. Biomim.* **9**, 016014. doi:10.1088/1748-3182/9/1/016014
- Crane, R. L., Cox, S. M., Kisare, S. A. and Patek, S. N.** (2018). Smashing mantis shrimp strategically impact shells. *J. Exp. Biol.* **221**, jeb176099. doi:10.1242/jeb.176099
- Daniel, T., Jordan, C. and Grunbaum, D.** (1992). Hydromechanics of swimming. In *Advances in Comparative and Environmental Physiology*, Vol. 11 (ed. R. McN. Alexander), pp. 17-49. London: Springer-Verlag.
- deVries, M. S.** (2017). The role of feeding morphology and competition in governing the diet breadth of sympatric stomatopod crustaceans. *Biol. Lett.* **13**, 20170055. doi:10.1098/rsbl.2017.0055
- deVries, M. S., Murphy, E. A. K. and Patek, S. N.** (2012). Strike mechanics of an ambush predator: the spearing mantis shrimp. *J. Exp. Biol.* **215**, 4374-4384. doi:10.1242/jeb.075317
- Diaz, G. A.** (1998). Description of the last seven pelagic larval stages of *Squilla* sp. (Crustacea, Stomatopoda). *Bull. Mar. Sci.* **62**, 753-762.
- Feller, K. D., Cronin, T. W., Ah Yong, S. T. and Porter, M. L.** (2013). Morphological and molecular description of the late-stage larvae of *Alima* Leach, 1817 (Crustacea: Stomatopoda) from Lizard Island, Australia. *Zootaxa* **3722**, 22-32. doi:10.11646/zootaxa.3722.1.2
- Fisher, R., Leis, J. M., Clark, D. L. and Wilson, S. K.** (2005). Critical swimming speeds of late-stage coral reef fish larvae: variation within species, among species and between locations. *Mar. Biol.* **147**, 1201-1212. doi:10.1007/s00227-005-0001-x
- Gohar, H. A. F. and Al-Kholy, A. A.** (1957). The larval stages of three stomatopod Crustacea. *Publ. Mar. Biol. Stat. Al-Ghardaqa*. **9**, 85-130.
- Green, P. A., McHenry, M. J. and Patek, S. N.** (2019). Context-dependent scaling of kinematics and energetics during contests and feeding in mantis shrimp. *J. Exp. Biol.* **222**, jeb198085. doi:10.1242/jeb.198085
- Greenwood, J. D. and Williams, B. G.** (1984). Larval and early post-larval stages in the abbreviated development of *Heterosquilla tricarinata* (Claus, 1871) (Crustacea, Stomatopoda). *J. Plankton Res.* **6**, 615-635. doi:10.1093/plankt/6.4.615
- Gronenberg, W.** (1996). Fast actions in small animals: springs and click mechanisms. *J. Comp. Physiol. A*. **178**, 727-734. doi:10.1007/BF00225821
- Hamano, T. and Matsuura, S.** (1987). Egg size, duration of incubation, and larval development of the Japanese mantis shrimp in the laboratory. *Nippon Suisan Gakkaishi* **53**, 23-39. doi:10.2331/suisan.53.23
- Hamlet, C., Strychalski, W. and Miller, L.** (2020). Fluid dynamics of ballistic strategies in nematocyst firing. *Fluids* **5**, 20. doi:10.3390/fluids5010020
- Harrison, J. S., Porter, M. L., McHenry, M. J., Robinson, H. E. and Patek, S. N.** (2020). Scaling and development of elastic mechanisms: the tiny strikes of larval mantis shrimp. *Dryad*. doi:10.5061/dryad.3n5tb2r7
- Haug, C. and Haug, J. T.** (2014). Defensive enrolment in mantis shrimp larvae (Malacostraca: Stomatopoda). *Contrib. Zool.* **83**, 185-194. doi:10.1163/18759866-08303003
- Haug, C., Ah Yong, S. T., Wiethase, J. H., Olesen, J. and Haug, J. T.** (2016). Extreme morphologies of mantis shrimp larvae. *Nauplius* **24**, e2016020. doi:10.1590/2358-2936e2016020
- Huxley, A. F.** (1957). A theory of muscular contraction. *Prog. Biophys. Biophys. Chem.* **7**, 255-318. doi:10.1016/S0096-4174(18)30128-8
- Ilton, M., Bhamla, M. S., Ma, X., Cox, S. M., Fitchett, L. L., Kim, Y., Koh, J.-S., Krishnamurthy, D., Kuo, C.-Y., Temel, F. Z. et al.** (2018). The principles of cascading power limits in small, fast biological and engineered systems. *Science* **360**, eaao1082. doi:10.1126/science.aao1082
- Kagaya, K. and Patek, S. N.** (2016). Feed-forward motor control of ultrafast, ballistic movements. *J. Exp. Biol.* **219**, 319-333. doi:10.1242/jeb.130518
- Larabee, F. J., Gronenberg, W. and Suarez, A. V.** (2017). Performance, morphology and control of power-amplified mandibles in the trap-jaw ant *Myrmoterias* (Hymenoptera: Formicidae). *J. Exp. Biol.* **220**, 3062-3071. doi:10.1242/jeb.156513
- Larabee, F. J., Smith, A. A. and Suarez, A. V.** (2018). Snap-jaw morphology is specialized for high-speed power amplification in the Dracula ant, *Myrmiotermes camillae*. *R. Soc. Open Sci.* **5**, 181447. doi:10.1098/rsos.181447
- Liang, X. and Crosby, A. J.** (2020). Uniaxial stretching mechanics of cellular flexible metamaterials. *Extreme Mech. Lett.* **35**, 100637. doi:10.1016/j.eml.2020.100637
- Longo, S. J., Cox, S. M., Azizi, E., Ilton, M., Olberding, J. P., St Pierre, R. and Patek, S. N.** (2019). Beyond power amplification: latch-mediated spring actuation is an emerging framework for the study of diverse elastic systems. *J. Exp. Biol.* **222**, jeb197889. doi:10.1242/jeb.197889
- Longo, S. L., Ray, W., Farley, G. M., Harrison, J., Jorge, J., Kaji, T., Palmer, A. R. and Patek, S. N.** (2021). Snaps of a tiny amphipod push the boundary of ultrafast, repeatable movement. *Curr. Biol.* **31**, R116-R117. doi:10.1016/j.cub.2020.12.025
- Marsh, R. L.** (1994). Jumping ability of anuran amphibians. *Adv. Vet. Sci. Comp. Med.* **38B**, 51-111.
- McHenry, M. J., Azizi, E. and Strother, J. A.** (2003). The hydrodynamics of locomotion at intermediate Reynolds numbers: undulatory swimming in ascidian larvae. *J. Exp. Biol.* **206**, 327-343. doi:10.1242/jeb.00069
- McHenry, M. J., Anderson, P. S. L., Van Wassenbergh, S., Matthews, D. G., Summers, A. P. and Patek, S. N.** (2016). The comparative hydrodynamics of rapid rotation by predatory appendages. *J. Exp. Biol.* **219**, 3399-3411. doi:10.1242/jeb.140590
- Meijering, E., Dzyubachyk, O. and Smal, I.** (2012). Methods for cell and particle tracking. *Methods Enzymol.* **504**, 183-200. doi:10.1016/B978-0-12-391857-4.00009-4
- Morgan, S. G. and Goy, J. W.** (1987). Reproduction and larval development of the mantis shrimp *Gonodactylus bredini* (Crustacea: Stomatopoda) maintained in the laboratory. *J. Crustacean Biol.* **7**, 595-618. doi:10.2307/1548646
- Morgan, S. G. and Provenzano, A. J.** (1979). Development of pelagic larvae and postlarva of *Squilla empusa* (Crustacea, Stomatopoda) with an assessment of larval characters within the Squillidae. *Fish. Bull.* **77**, 61-90.
- Nüchter, T., Benoit, M., Engel, U., Özbek, S. and Holstein, T. W.** (2006). Nanosecond-scale kinetics of nematocyst discharge. *Curr. Biol.* **16**, R316-R318. doi:10.1016/j.cub.2006.03.089
- Olberding, J. P., Deban, S. M., Rosario, M. V. and Azizi, E.** (2019). Modeling the determinants of mechanical advantage during jumping: consequences for spring- and muscle-driven movement. *Integr. Comp. Biol.* **59**, 1515-1524. doi:10.1093/icb/icz139
- Palecanda, S., Feller, K. D. and Porter, M. L.** (2020). Using larval barcoding to estimate stomatopod species richness at Lizard Island, Australia for conservation monitoring. *Sci. Rep.* **10**, 10990. doi:10.1038/s41598-020-67696-x
- Patek, S. N.** (2019). The power of mantis shrimp strikes: interdisciplinary impacts of an extreme cascade of energy release. *Integr. Comp. Biol.* **59**, 1573-1585. doi:10.1093/icb/icz127
- Patek, S. N., Korff, W. L. and Caldwell, R. L.** (2004). Deadly strike mechanism of a mantis shrimp. *Nature* **428**, 819-820. doi:10.1038/428819a
- Patek, S. N., Nowroozi, B. N., Baio, J. E., Caldwell, R. L. and Summers, A. P.** (2007). Linkage mechanics and power amplification of the mantis shrimp's strike. *J. Exp. Biol.* **210**, 3677-3688. doi:10.1242/jeb.006486
- Porter, M. L., Zhang, Y., Desai, S., Caldwell, R. L. and Cronin, T. W.** (2010). Evolution of anatomical and physiological specialization in the compound eyes of stomatopod crustaceans. *J. Exp. Biol.* **213**, 3473-3486. doi:10.1242/jeb.046508
- Provenzano, A. J. and Manning, R. B.** (1978). Studies on development of stomatopod Crustacea II. The later larval stages of *Gonodactylus oerstedii* hansen reared in the laboratory. *Bull. Mar. Sci.* **28**, 297-315.
- Pyne, R. R.** (1972). Larval development and behaviour of the mantis shrimp, *Squilla armata* Milne Edwards (Crustacea: Stomatopoda). *J. R. Soc. N. Z.* **2**, 121-146. doi:10.1080/03036758.1972.10429369
- Robinson, H. E., Strickler, J. R., Henderson, M. J., Hartline, D. K. and Lenz, P. H.** (2019). Predation strategies of larval clownfish capturing evasive copepod prey. *Mar. Ecol. Prog. Ser.* **614**, 125-146. doi:10.3354/meps12888
- Rosario, M. V. and Patek, S. N.** (2015). Multilevel analysis of elastic morphology: the mantis shrimp's spring. *J. Morph.* **276**, 1123-1135. doi:10.1002/jmor.20398
- Rosario, M. V., Sutton, G. P., Patek, S. N. and Sawicki, G. S.** (2016). Muscle-spring dynamics in time-limited, elastic movements. *Proc. R. Soc. B* **283**, 20161561. doi:10.1098/rspb.2016.1561
- Sakes, A., van der Wiel, M., Henselmans, P. W. J., van Leeuwen, J. L., Dodou, D. and Breedveld, P.** (2016). Shooting mechanisms in nature: a systematic review. *PLoS ONE* **11**, e0158277. doi:10.1371/journal.pone.0158277
- Schneider, C. A., Rasband, W. S. and Eliceiri, K. W.** (2012). NIH image to ImageJ: 25 years of image analysis. *Nat. Methods* **9**, 671-675. doi:10.1038/nmeth.2089
- Seid, M. A., Scheffrahn, R. H. and Niven, J. E.** (2008). The rapid mandible strike of a termite soldier. *Curr. Biol.* **18**, R1049-R1050. doi:10.1016/j.cub.2008.09.033
- Shanbhogue, S. L.** (1978). The embryonic and early larval development of *Gonodactylus falcatus* (Forsskal) (Crustacea: Stomatopoda) from India. *J. Mar. Biol. Assoc. India.* **20**, 86-97.
- Sutton, G. P., Mendoza, E., Azizi, E., Longo, S. J., Olberding, J. P., Ilton, M. and Patek, S. N.** (2019). Why do large animals never actuate their jumps with

- latch-mediated springs? because they can jump higher without them. *Integr. Comp. Biol.* **59**, 1609-1618. doi:10.1093/icb/icz145
- Van Der Wal, C., Ah Yong, S. T., Ho, S. Y. W. and Lo, N.** (2017). The evolutionary history of Stomatopoda (Crustacea: Malacostraca) inferred from molecular data. *PeerJ* **5**, e3844. doi:10.7717/peerj.3844
- Vogel, S.** (1981). *Life in Moving Fluids*. Princeton, USA: Princeton University Press.
- Walker, G.** (2004). Swimming speeds of the larval stages of the parasitic barnacle, *Heterosaccus lunatus* (Crustacea: Cirripedia: Rhizocephala). *J. Mar. Biol. Assoc. U.K.* **84**, 737-742. doi:10.1017/S002531540400983Xh
- Wendt, D. E.** (2000). Energetics of larval swimming and metamorphosis in four species of *Bugula* (Bryozoa). *Biol. Bull.* **198**, 346-356. doi:10.2307/1542690
- Wiethase, J., Haug, J. T. and Haug, C.** (2020). Detailed description of some mantis shrimp larvae and their implication for the character evolution within Stomatopoda. *Nauplius* **28**, e2020001. doi:10.1590/2358-2936e2020001
- Williams, T. A.** (1994). A model of rowing propulsion and the ontogeny of locomotion in *Artemia* larvae. *Biol. Bull.* **187**, 164-173. doi:10.2307/1542239
- Zack, T. I., Claverie, T. and Patek, S. N.** (2009). Elastic energy storage in the mantis shrimp's fast predatory strike. *J. Exp. Biol.* **212**, 4002-4009. doi:10.1242/jeb.034801

Supplementary Materials:

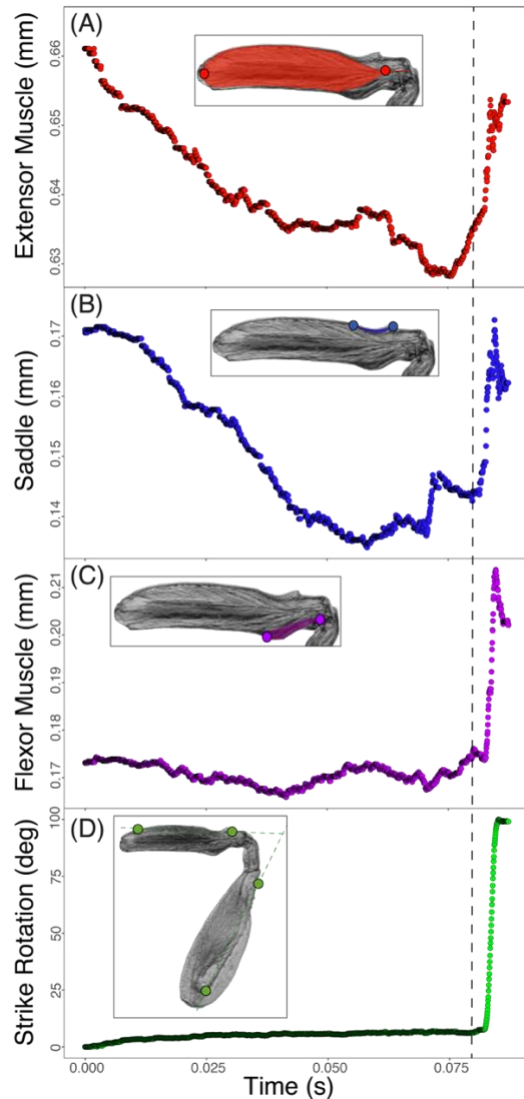


Figure S1. The synchronous and sequential timing of extensor muscle contraction, saddle shortening, flexor lengthening, and striking body rotation support the presence of LaMSA in larval mantis shrimp.

Shortening of the extensor muscles (A) occurs simultaneously with shortening of the saddle (B), which suggests that elastic energy is stored via exoskeletal deformation in larvae similarly to adult mantis shrimp. The lengthening of the flexor muscles (C) occurs prior to the onset of the strike (vertical dashed line). The rapid rotation of the striking body (D) occurs simultaneously with the recoil of the saddle and lengthening of the muscles. points overlaid on the appendage images represent the tracked points over the course of a single strike. Each graph represents the rotational or length changes based on the tracked points. The graphs show a spring actuated larval strike and indicate movement between frames from high speed imaging ($20,000 \text{ frames s}^{-1}$).

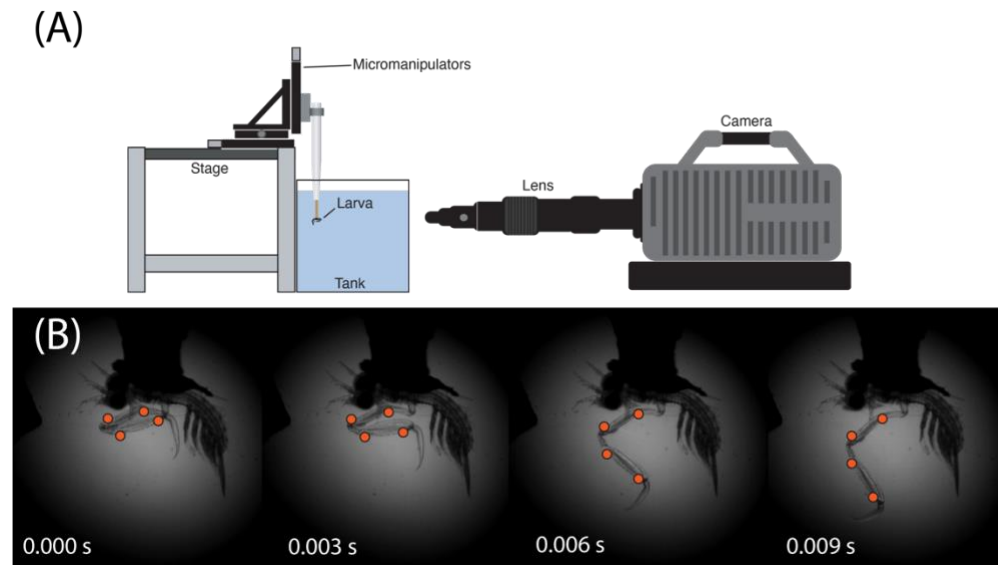


Figure S2: We developed a custom filming rig to collect and measure raptorial appendage strikes from larval *Gonodactylaceus falcatus*. (A) Each larva was affixed to a tooth pick and suspended in saltwater using a custom designed stage. (B) Four points along the raptorial appendage were tracked over the course of each strike in order to measure the angular displacement of the propodus relative to the merus over time. Orange circles represent tracked points.

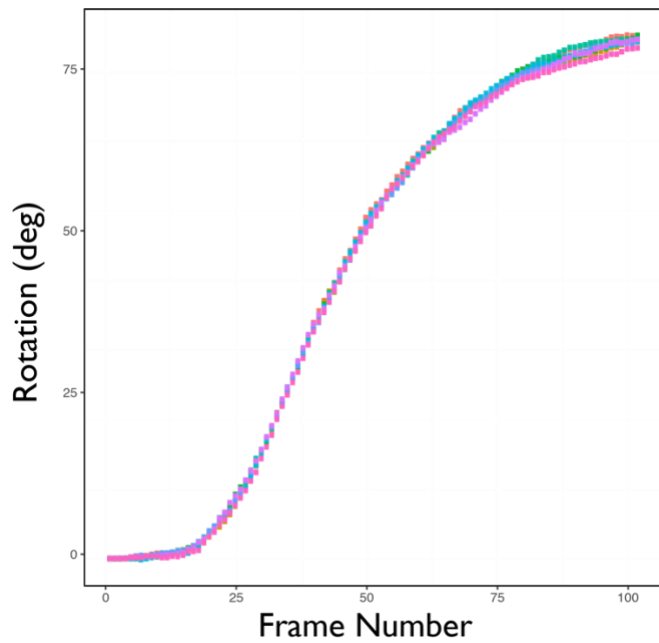
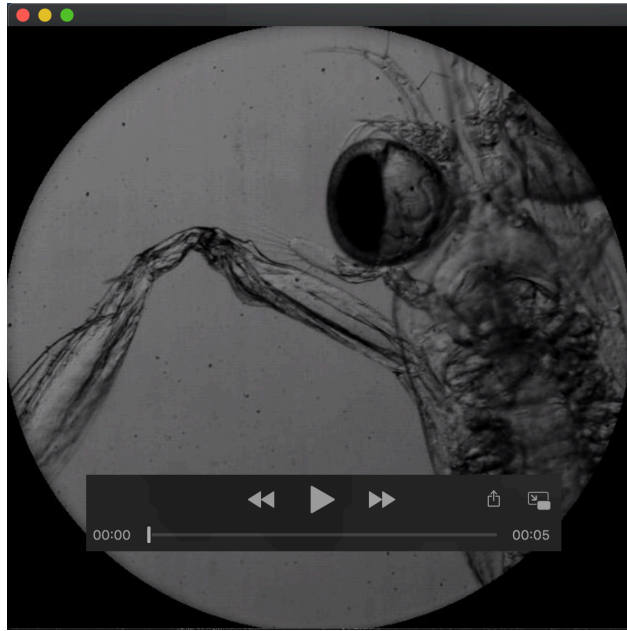


Figure S3: Characteristic strike of larval *G. falcatus* digitized ten times to measure tracking error. Each color represents the same strike but a different digitizing sequence.

Table S1. Peak swimming or prey capture speeds of larval organisms. The present study of larval mantis shrimp strike speed is highlighted in light gray.

[Click here to Download Table S1](#)



Movie 1: The LaMSA mechanism in the *Gonodactylaceus falcatus* larval raptorial appendage is revealed when placed under a microscope slide and filmed at 2,000 frames per second.



Movie 2: A characteristic raptorial appendage strike by *Gonodactylaceus falcatus* larva when fixed to toothpick and filmed at 20,000 frames per second.